COPY 1

DOT/FAA/CT-82/117

5

FEDERAL AVIATION ADMINISTRATION

APR 20 1983

TECHNICAL CENTER LIBRARY
ATLANTIC CITY, N.J. 08405

Effect of Volatility on Air-Fuel Ratio Distribution and Torque Output of A Carbureted Light Aircraft Piston Engine

Nat Won Sung
Kevin Morrison
Donald J. Patterson

The University of Michigan
Ann Arbor, Michigan 48109

March 1982

Final Report

This document is available to the U.S. public through the National Technical Information Service, Springfield, Virginia 22161.

US Department of Transportation
Federal Aviation Administration
Technical Center
Atlantic City Airport, N.J. 08405

FAA TECHNICAL CENTER LIBRARY NJ
University o/Effect of volatility on air
00008029

NOTICE

This document is disseminated under the sponsorship of the Department of Transportation in the interest of information exchange. The United States Government assumes no liability for the contents or use thereof.

The United States Government does not endorse products or manufacturers. Trade or manufacturer's names appear herein solely because they are considered essential to the object of this report.

Technical Report Documentation Page

1. Report No.	2. Government Accession No.	3. Recipient's Catalog No.
DOT/FAA/CT-82/117		

4. Title and Subtitle	5. Report Date
Effect of Volatility On Air-Fuel Ratio Distribution and Torque Output of a Carbureted Light Aircraft Piston Engine	September 1982
	6. Performing Organization Code
	8. Performing Organization Report No.
7. Author(s) D. Patterson, K. Morrison and Nak Won Sung	
9. Performing Organization Name and Address The University of Michigan Department of Mechanical Engineering 309 W.E. Lay Automotive Laboratory, North Campus Ann Arbor, Michigan 48109	10. Work Unit No. (TRAIS)
	11. Contract or Grant No. DOT-FA79NA-6083
12. Sponsoring Agency Name and Address Federal Aviation Administration Technical Center Atlantic City Airport, New Jersey 08405	13. Type of Report and Period Covered Final Report May 1981 - September 1982
	14. Sponsoring Agency Code

15. Supplementary Notes

16. Abstract

A comprehensive sea - level - static test cell data collection and evaluation effort to review operational characteristics of a carbureted light aircraft piston engine as related to fuel volatility and air-fuel ratio distribution to cylinders. Presented herein are results, data, and conclusions drawn from test cell engine operation on 100LL aviation grade fuel and various blends of automotive grade fuel.

Sea - level - static test cell engine operations were conducted utilizing an AVCO Lycoming O-320 engine connected to an eddy current dynamometer which facilitated data collection under various engine load conditions. Test cell instrumentation was utilized to obtain operational data (temperatures, pressures, flow rates, torque, horsepower, exhaust emissions, etc.) from idle through cruise to maximum power with fuel grades having reid vapor pressure of 6.7, 11.7 and 14.0. The primary purpose of test cell engine operation was to observe real-time performance characteristics associated with automotive grade fuel utilized by piston powered light general aviation aircraft. In fulfillment of this task, baseline engine operations were established with 100LL aviation grade fuel followed by two blends of automotive grade fuel.

17. Key Words		18. Distribution Statement
General Aviation	Fuel Additives	Document is available to the U.S. public through the National Technical Information Service, Springfield, VA 22161
Automotive Fuel	Light Aircraft	
Aviation Fuel	Piston Engines	

19. Security Classif. (of this report)	20. Security Classif. (of this page)	21. No. of Pages	22. Price
Unclassified	Unclassified		

Form DOT F 1700.7 (8-72) Reproduction of completed page authorized

TABLE OF CONTENTS

Page

EXECUTIVE SUMMARY v

INTRODUCTION.....1

Background.....1
Relevant Literature.....2

EXPERIMENTATION.....2

Equipment 2
Procedures.....11
Results.....13

DISCUSSION.....14

CONCLUSIONS.....20

REFERENCES.....24

APPENDIX A - STOICHIO METRIC AIR-FUEL RATIO CALCULATION

APPENDIX B - DATA COLLECTED FROM EXPERIMENT

LIST OF FIGURES

		page
1.	Distribution of Fuel Components	3
2.	Average Cylinder Deviation for Concentration of Various Fuel Components in Fuel	3
3.	A Schematic View of the Experimental Setup	5
4.	Distillation Curve for All Fuels Tested	10
5.	Torque Variation Output Signal (Test Fuel 15B)	14
6.	Standard Deviation of Torque Variation Produced with Each Tested Fuel	15
7.	Air-Fuel Ratio Distribution with Baseline (100LL) and Test Fuel 15B	16
8.	Air-Fuel Ratio Distribution with Baseline (100LL) and Test Fuel 12A	17
9.	Brake Specific Fuel Consumption Rate with Each Fuel Tested	20
10.	Throttle Plate and Intake Air Temperature Variation with Each Fuel Tested	21
11.	Fuel Pressure at the Carburetor and Temperatures at Various Locations with Baseline (100LL) and 15B Test Fuel	22

EXECUTIVE SUMMARY

This report "Effects of Volatility on Air-Fuel Ratio Distribution and Torque Output of a Carbureted Light Aircraft Piston Engine" represents observations/data obtained by the The University of Michigan for the FAA Technical Center under contract DOT-FA79NA-6083. As part of the contract effort, the university conducted test cell engine testing of an FAA Technical Center provided AVCO Lycoming 0-320 light aircraft piston engine. Data was obtained on engine operational performance, cylinder-to-cylinder air-fuel distribution, exhaust emissions and maldistribution associated with 100LL aviation grade fuel and two blends of automotive fuel with a reid vapor pressure of 11.7 and 14.0.

Standard engine test cycles were established which encompassed flight conditions such as; idle, full power, cruise (rich and lean), descent and approach. These test cycles were utilized for testing all fuels and led to the following conclusions:

1. Mixture distribution and specific fuel consumption were similar with all fuels tested.

2. Power output/torque fluctuations for all fuels were about the same.

3. While actual vapor lock did not manifest itself during engine testing, fuel system pressure and volume flow rate fluctuations associated with the higher volatility automotive fuel indicated an increase in vapor formation which would ultimately induce vapor lock.

INTRODUCTION

BACKGROUND

For the aircraft piston engine, safety, performance, and durability are principal concerns. In recent years, the price of aviation gasoline has increased sharply and some temporary shortages have arisen. As a result, there has been increased interest in the potential suitability of automobile gasoline for light aircraft. To address this question, a comprehensive study of the existing literature on fuel related problems in both aviation and automotive engines has been performed at the University of Michigan by Patterson et al. (reference 1). Several potential problems for use of autogas in light aircraft were identified and classified as either short-term or long-term in nature. Knock, preignition, vapor lock, carburetor icing, and hot restart were identified as potential short-term problems. Loss of performance due to maldistribution, valve sticking, material degradation, lubrication, wear, and fuel storage stability were identified as potential long-term problems. The problems of vapor lock, icing, and maldistribution are directly related to fuel volatility.

Volatility affects engine performance through its influence on the degree of fuel evaporation in the fuel delivery system, intake manifold, and cylinder prior to the combustion process. The American Society for Testing and Materials (ASTM) distillation process 90 percent point temperature indicates the amount of heavy components in the gasoline, and the 10 percent point temperature indicates the amount of light components. Since automobile gasolines have higher ASTM 90 percent point temperatures and lower 10 percent point temperatures than aviation gasolines, it was expected that aviation engines would exhibit increased maldistribution when automobile gasoline was used.

This report summarizes the first portion of an experimental program to assess some aspects of autogas use in an Avco Lycoming O-320 engine. Reported herein are the development of the experimental facility and an initial evaluation using autogas type fuels of varying volatility. Determined in this program were the degree of maldistribution and the resulting torque variability of these autogas fuels compared to commercial avgas.

Two autogas fuels of different volatility were compared with commercial 100LL avgas. Their 10 percent point temperatures were 105 and 89° F; 50 percent temperatures, 226 and 169° F; 90 percent temperatures, 329 and 338° F; and Reid vapor pressures, 11.7 and 14.0 pounds per square inch. A test matrix was selected consisting of engine operating points representative of a production aircraft installation. The speed ranged from 1000 to 2700 revolutions per minute and load from 8 to 160 horsepower. The mixture ratio in each cylinder was determined using a Lamdascan air-fuel ratio meter. The torque variation was determined by a strain gage type torque sensor located in the driveshaft between the flywheel and dynamometer. Standard engine data, such as temperatures, pressures, fuel consumption, and power output were recorded also.

RELEVANT LITERATURE

Maldistribution is known to decrease power output while increasing fuel consumption. Yu (reference 2) measured cycle-to-cycle and cylinder-to-cylinder air-fuel ratio variations in a V-8 engine using the Orsat exhaust gas analysis method and gas chromatography method (reference 3). From his data, he correlated the variance of mixture distribution with power and economy loss. He found maldistribution even for gaseous mixtures of propane and air. In his study, he showed that inducing swirl and extending the mixing length improved distribution. Donahue and Kent (reference 4) found that the design of the intake air manifold runners could alter the mixture distribution patterns more than could engine speed, mixture temperature, or fuel volatility. In an aircraft engine, it may be anticipated from the literature, that poor distribution will cause rough running and result in more stress in the propeller and crank assembly and lead to power and economy losses.

Maldistribution can also lead to knocking in one or more cylinders due to maldistribution of antiknock additives and individual knock resistant fuel components. Cooper et al. (reference 5) studied the distribution of both whole fuels and their individual components in several V-8 engines. They used an exhaust gas analyzer of the catalytic-cell type to determine fuel distribution, and a radioactive tracer method using radioactive hydrogen (tritium) or carbon-14 for detecting maldistribution of individual fuel components. Figure 1 shows the maldistribution of five fuel components of a whole fuel. They concluded that maldistribution depended primarily on the boiling temperature of the component. Figure 2 summarizes their results. Let us assume that a 100 percent increase in average concentration deviation (figure 2) defines the upper limit of "acceptable" maldistribution. The boiling temperature range associated with that is shown by the horizontal bar at 5.4 percent average deviation. The boiling temperature range for good distribution is then from about 150 to 300° F. From the foregoing, it may be expected that increasing light end or decreasing heavy end fuel volatility will increase maldistribution since more light and heavy components are present in the fuel.

In a previous study with the O-320 engine, Mirsky and Nicholls (reference 6) studied the effects of cylinder-to-cylinder mixture distribution on emissions with a turbulent flow manifold. Their results showed that a turbulent flow manifold produced an improvement in distribution for the low power operating modes but a deterioration for the high power modes.

EXPERIMENTATION

EQUIPMENT

The Avco Lycoming O-320 engine was used for the experimental study. This was a four-cylinder engine which originally was equipped with a

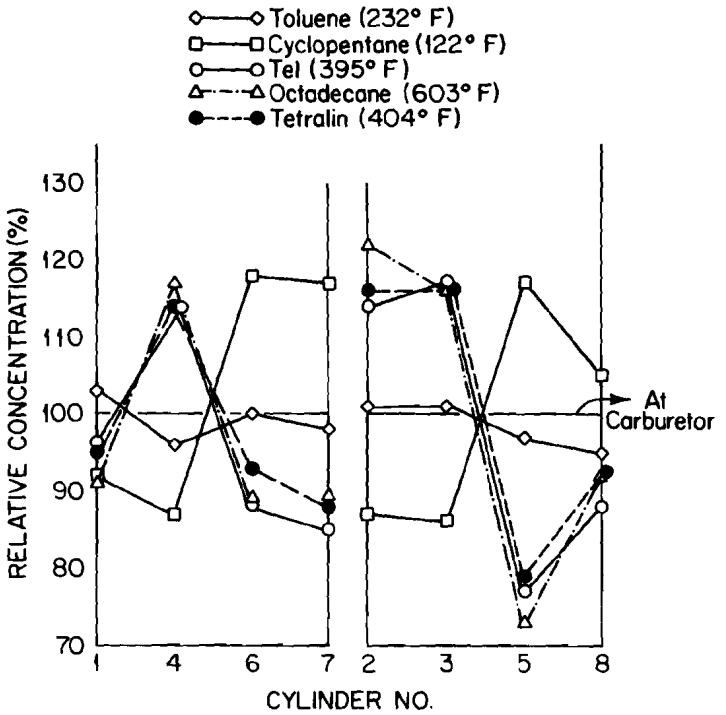

FIGURE 1. DISTRIBUTION OF FUEL COMPONENTS
Values in parentheses are boiling temperatures of the pure components. (V-8 truck engine at 2400 rpm, 40° throttle, from reference 5)

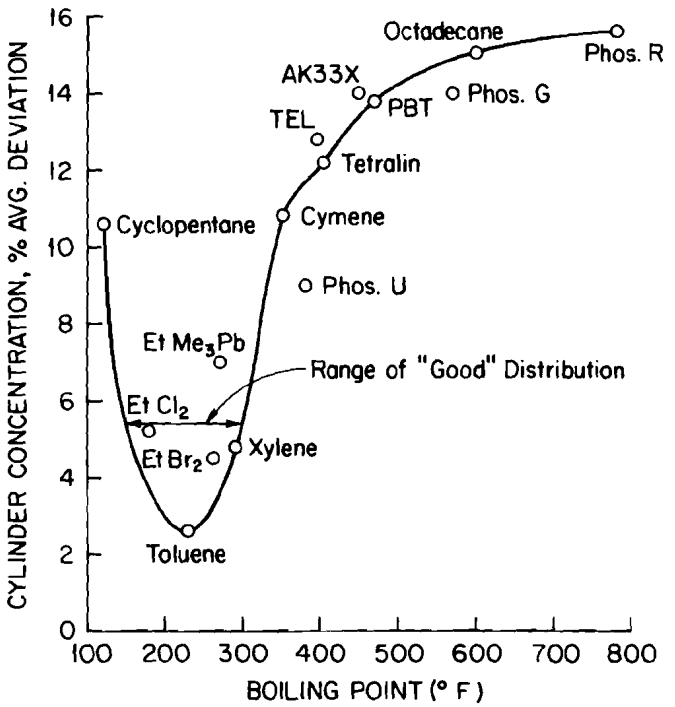

FIGURE 2. AVERAGE CYLINDER DEVIATION FOR CONCENTRATION OF VARIOUS FUEL COMPONENTS IN FUEL (V-8 truck engine at 2400 rpm, 40° throttle, from reference 5)

fuel injection system. For this study, the fuel injection system was replaced by a carburetor[1] and intake manifold. On this engine, the carburetor was located below the engine and intake manifold runners. The updraft design draws the mixture upward through runners that pass through the oil sump. The characteristics of this engine are listed in table 1.

TABLE 1. CHARACTERISTICS OF THE AVCO LYCOMING O-320 ENGINE

Rated horsepower	160
Rated speed, rpm	2700
Bore, inches	5.125
Stroke, inches	3.875
Displacement, cubic inches	319.8
Compression ratio	8.5:1
Firing order	1-4-2-3
Spark timing, degrees BTC	25
Propeller drive ratio	1:1
Propeller drive rotation (from rear view)	C-Clockwise
Octane requirement	90-97

In place of the usual propeller, a flywheel of 17 inch diameter and 2.1 inch thickness was installed to provide a proper amount of inertia. The flywheel was connected to a dynamometer by a driveshaft. An eddy current dynamometer was used to apply different loads to the engine. The dynamometer load was measured by a Link unibeam pneumatic load cell. Between the flywheel and driveshaft, an inline Lebow Model 1239-12K shaft torque sensor was installed to measure torque variation. The torque sensor provided a voltage output proportional to the torque on the driveshaft. A centrifugal blower driven by a 20 HP motor was used to cool the engine. Thermocouples and pressure taps were located at various places on the engine and test equipment as indicated in figure 3 and listed in table 2. These measured fuel, oil, and air system conditions. One thermocouple was installed about a half inch downstream

[1] Marvel Schebler aircraft carburetor, model MA-4SPA, part # 10-5009N, serial # BL 20 13530

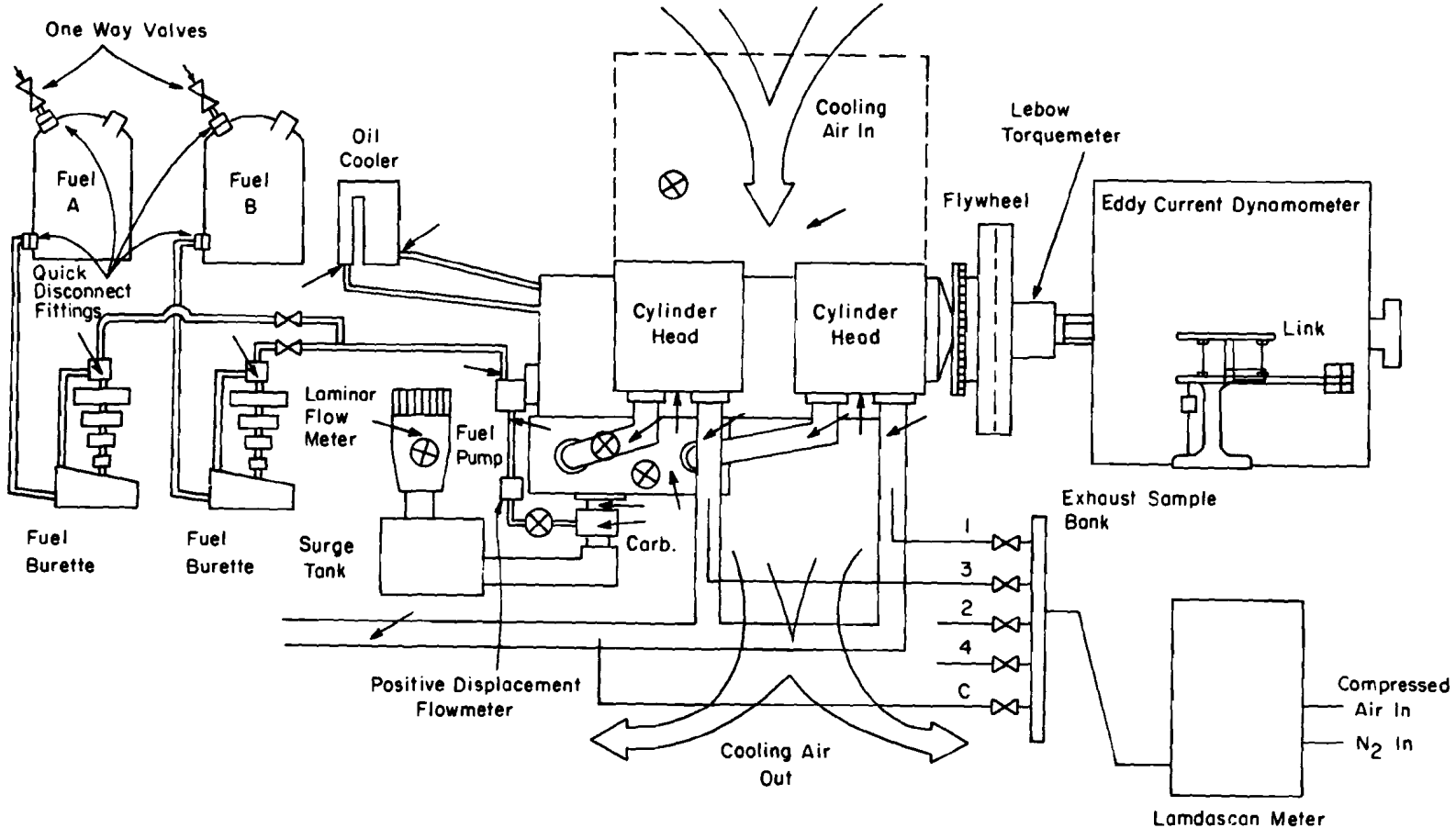

FIGURE 3. A SCHEMATIC VIEW OF THE EXPERIMENTAL SETUP (↗ Locations of the Thermocouples, ⊗ Locations of Pressure Measurement)

TABLE 2. INSTRUMENTATION

Pressure:

Differential pressure across air flowmeter, by micromanometer in inches of H_2O

Cooling air pressure before engine, by manometer in inches of H_2O

Intake manifold vacuum, by manometer in inches of Hg

Fuel pressure at carburetor inlet fitting, by Bourdon gage in psi

Oil pressure, by Bourdon gage in psi

Thermocouples:

Individual exhaust gas temperatures (4 cylinders)
Oil into heat exchanger
Oil out of heat exchanger
Oil inside sump
Carburetor fuel bowl
Fuel pump inlet
Fuel pump outlet
Fuel burette
Laminar airflow meter
Carburetor base-in airstream near throttle plate
Mixture stream of individual intake manifold tubes (4 cylinders)
Cylinder head (4 cylinders)

Other:

Positive displacement fuel flow sensor
Burette type volumetric fuel flowmeter (2)
Meriam laminar airflow meter
Lamdascan air-fuel ratio meter
Lebow inline torque sensor
Eddy current dynamometer
Link pneumatic load cell
Nicolet Model 206 digital oscilloscope
Hewlett Packard Model 9830 computer
Digital voltmeter

of the throttle plate as one indication of potential icing problems. This temperature is termed throttle plate temperature. A thermocouple in the laminar flowmeter was used to indicate ambient temperature. A duel system was installed to permit an instantaneous change of test fuels while running the engine. Each fuel system employed a 5 gallon fuel can, an electrically activated valve, and a Testron Model 1548 volumetric burette for fuel flow measurement. In addition, a Brooks-Micro Oval II Model LS-41 positive displacement fuel flowmeter was placed in the line between the fuel pump and carburetor. In actual operation, due to the vapor formed in this part of the fuel system, the Brooks fuel flowmeter output was erratic and therefore the resulting data was not utilized.

The volumetric flowrate of engine intake air was calculated from the pressure drop across a Meriam Model 50MC2-4SF laminar flowmeter. Between the air meter and the engine, a surge tank of 1 cubic foot with a blowout panel was placed to dampen intake air pulsations and to protect against possible backfires into the intake system. To control lubricating oil temperature, an external oil cooler was installed.

To study mixture distribution, a Lamdascan air-fuel ratio meter manufactured by Sensors Incorporated was used. This unit measures air-fuel ratio by measuring exhaust oxygen content. In operation, an exhaust sample is mixed with a known proportion of air which is then passed over a platinum catalyst in order to react all carbon monoxide, hydrocarbons, hydrogen, and aldehydes to products of complete combustion. The resulting product stream contains only water vapor, carbon dioxide, oxygen, nitrogen, and nitric oxides. The oxygen concentration of this stream is measured by a zirconia sensor. The zirconia sensor consists of porous platinum electrodes over a porous ZrO_2-ceramic electrolyte which separates the sample gas from the ambient air reference gas. Due to the difference of oxygen concentration in the two gases, an electrochemical reaction takes place resulting in electron flow. A voltage is generated which is related to the exhaust oxygen concentration according to the Nernst equation (reference 7),

$$E = 2.303 \frac{RT}{4F} \log_{10} \frac{O_2}{21} \tag{1}$$

where

E = Generated voltage, volts

R = Universal gas constant, 1.986 cal/gmol $^{\circ}$ K

F = Faraday constant, 23060 cal/volts

T = Temperature of sensor, $^{\circ}$ K

O_2 = Exhaust oxygen, percent

From the oxygen concentration of the exhaust and the H/C ratio of the fuel, the equivalence ratio of the exhaust is calculated by equation (2).

$$\phi = 1 + \frac{(4.76C - X)\ (1 + 0.302n)}{(1 - 4.76C)\ (1 + 0.250n)} \qquad (2)$$

where

ϕ = Equivalence ratio

n = H/C ratio (This equation is relatively insensitive to the range of H/C ratios for most gasolines.)

C = O_2 fraction in sample gas

X = Doping rate for dilution of the exhaust sample with air

In order to ensure that all the unreacted products of combustion are reacted on the catalyst and not on the sensor when measuring samples richer than stoichiometric, a heated capillary allows addition of a known fraction of oxygen to the sample stream. The response time of the Lamdascan meter is less than 300 milli-seconds (reference 8). For taking the exhaust sample from each cylinder, an exhaust sampling manifold was constructed. The cylinder to be sampled was selected by an electrically operated valve on the sampling manifold. Samples were taken 3.4 inches downstream from each exhaust port flange.

For measuring and recording the torque outputs from the Lebow torque sensor, a Nicolet Model 206 digital oscilloscope was used. This model had a magnetic diskette storage unit. This unit was interfaced to a Hewlett Packard Model 9830 computer which was used to calculate the standard deviation of the torque output.

For this study, two special fuels were prepared by the Phillips Petroleum Company. Their properties, as measured by the Ethyl Corporation Laboratories and by the Phillips Petroleum Company, are listed in table 3. The differences in RVP and distillation temperature data between laboratories indicate a small loss of light fuel components during the shipping, handling, and sampling. The octane ratings for two autogases were sufficiently high to meet the octane requirement of the engine.

The distillation curves for the three tested fuels are plotted in figure 4. The 10 percent distillation temperature is the lowest for the 15 RVP fuel and the highest for the aviation fuel. The range of U. S. summer and winter autogas for 1979 is also indicated (references 9 and 10) in figure 4. In this figure, the estimated range of good distribution from figure 2 is indicated for each fuel.

TABLE 3. PROPERTIES OF TESTED FUELS

	100LL Avgas	12A Autogas	15B Autogas
H/C	0.185	0.162	0.175
RVP	6.7	11.7 (12.1)*	14.0 (15.0)
MON	101.55	90.66 (91.2)	90.01
RON	104.14	99.57 (100.0)	99.57
Distillation temperature (° F)			
IBP	108	84 (85)	80 (80)
5%	129	93 (97)	84 (87)
10	148	105 (112)	89 (94)
15	162	118 (127)	95 (100)
20	175	134 (143)	101 (105)
30	194	172 (182)	116 (120)
40	207	205 (212)	137 (144)
50	213	226 (231)	169 (180)
60	218	243 (248)	211 (220)
70	223	263 (268)	242 (251)
80	230	290 (296)	279 (290)
90	244	329 (334)	338 (349)
95	260	361 (372)	368 (386)
FBP	334	415 (420)	412 (419)
Recovery (ml)	98.0	96.4 (96.6)	96.5 (97.4)
Residue (ml)	0.1	0.3 (0.5)	0.1 (0.8)
Loss (ml)	1.9	3.3 (2.9)	3.4 (1.8)
TEL (ml/gal)	-	- (3.0)	- (3.0)
A/F at stoich.**	15.01	14.63	14.85
S. G.***	0.7047	0.7389	0.704

* Data in the parenthesis are from the Phillips Petroleum Co., measured before shipment.

** Calculated (Calculation procedures are shown in Appendix A)

*** Specific gravity measured at the Automotive Laboratory of the University of Michigan

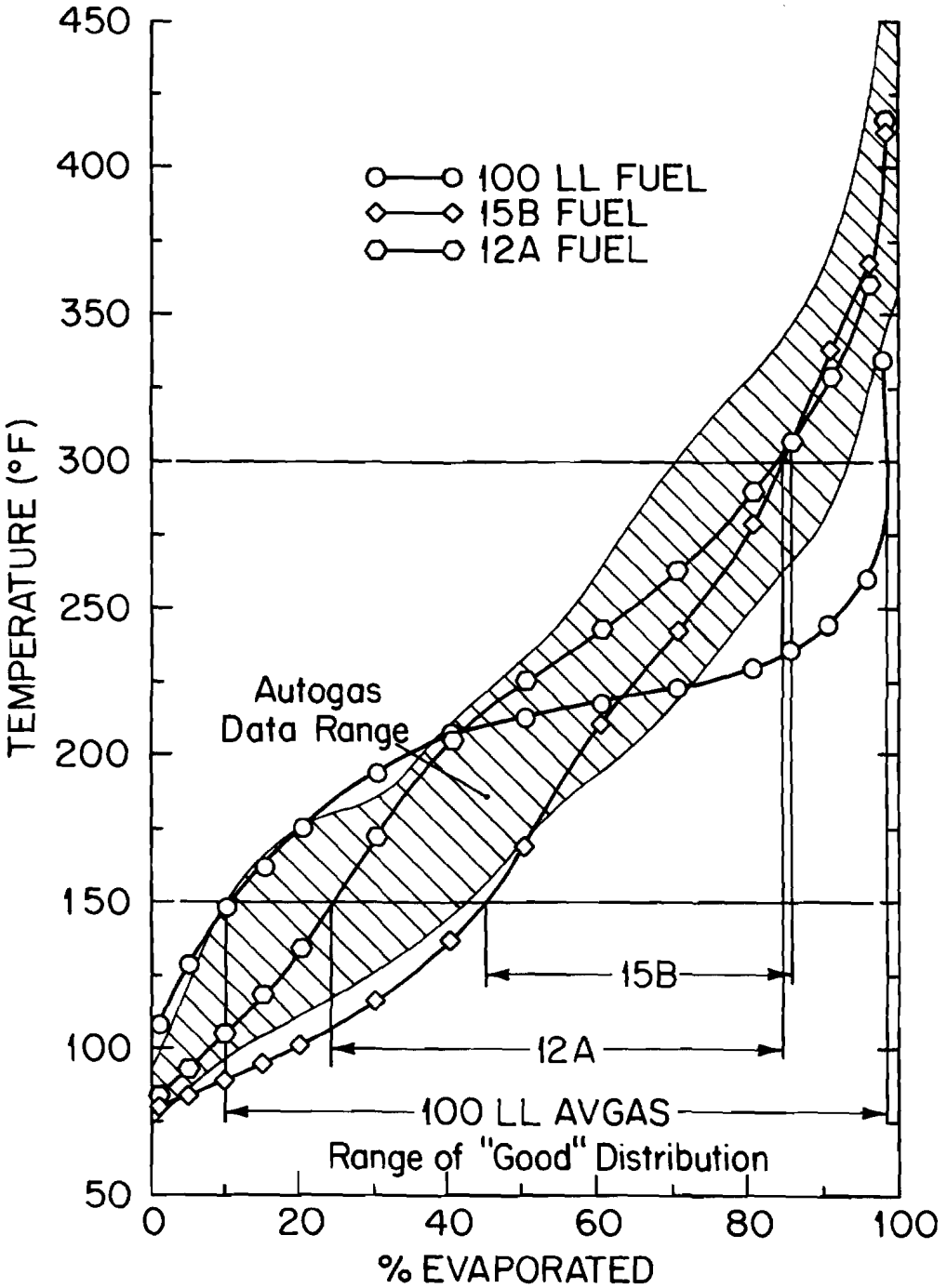

FIGURE 4. DISTILLATION CURVES FOR ALL FUELS TESTED
-Ethyl Laboratory data

In order to keep the highly volatile components in the fuel, each fuel was kept sealed in its barrel until it was transferred to the fuel cans. The barrel and fuel cans were equipped with self-sealing, quick disconnect hose fittings for the supply and vapor return lines. The fuel flowed by gravity from the barrel and entered the bottom of the fuel can through these flexible lines and any fuel vapor and displaced air were returned to the barrel through the return line.

The fuel flowrate from the cans to the engine was measured by a volumetric burette. This had a clock, electric switching unit and 4 different volume reservoirs. Since fuel consumption increased sharply with increased engine load and speed, larger reservoirs were used for the higher engine speeds in order to obtain large enough measuring intervals for accurate volumetric flowrate determination.

PROCEDURES

The engine was started and warmed up on 100LL avgas until reaching stable operation. Cylinder head temperatures were monitored and kept below 450° F by manually controlling the amount of cooling air from the blower. For taking data, a test matrix of 8 different speed and load conditions was selected from the propeller horsepower curves at sea level published in the engine operating manual (reference 11). These are listed in table 4. The test points represent various modes of operation including idle, cruise, approach, decent and maximum power for a takeoff. At all of these points, the engine was operated at full rich mixture settings. To simulate economy cruise operation at 2200 and 2350 rpm, a lean mixture was used also. The mixture was controlled by the manually operated knob which adjusted the main metering jet. Lean mixtures were set by leaning to approximately a stoichiometric ratio as indicated by the Lamdascan air-fuel ratio meter for the overall exhaust sample.

For each speed and load condition, data were taken for 100LL fuel first and then the fuel was immediately switched to the test fuel and the engine allowed to stabilize. The data collected included various temperatures and pressures and the time required to consume a fixed volume of fuel. Due to the time required to finish one test matrix, two runs of the test matrix, one for 100LL and one for 15B fuel were collected on one day and the other two runs for 100LL and 12A fuel were collected on the next day. For convenience, the data was collected in order of increasing rpm. This allowed attainment of stabilized operation in a minimum time for minimum test fuel consumed and less wear and tear on the test engine, particularly at the higher power settings.

From the air-fuel ratio meter, the exhaust sample oxygen concentration for each cylinder was read as an average voltage on a digital voltmeter. The torque signal from the shaft torque sensor was found to have a low frequency noise of 6.7 Hertz which arose from the natural frequency of driveshaft and flywheel combination. To circumvent this noise, a band pass filter, 20 to 500 Hz, was used. The spark voltage for number 1 cylinder was used to indicate the relative phasing of the torque output

TABLE 4. ENGINE TEST CONDITIONS

Mode	RPM	HP
1. Idle	1000	8
2. Normal approach	1600	32
3. Normal decent	2000	65
4. Economy cruise, rich	2200	87
5. Economy cruise, lean	2200	87
6. Normal cruise, rich	2350	107
7. Normal cruise, lean	2350	107
8. Maximum power	2700	160

with the individual cylinder power strokes.

RESULTS

In this section, the results of the study are presented. The detailed data has been included in appendix B. Figure 5 shows the torque variations for 100LL fuel at 2200 rpm and 87 HP. In this figure, the DC part of the signal was removed by the band pass filter. The average torque level was measured with the link load cell attached to the dynamometer. From the torque variation data, the standard deviation for torque was calculated.

$$\text{Standard deviation of torque} = [\{\sum_{i=1}^{N} (T_i - T)^2\}/(N-1)]^{1/2} \qquad (3)$$

where T is the average value of torque.

For this, 500 values (N=500) were used for all calculations.

The standard deviation of torque at different speeds and loads is plotted in figure 6. Since the experiments comparing 100LL with 15B fuel and 100LL with 12A fuel were carried out on two days and therefore under somewhat different ambient temperatures, these data are plotted separately. These temperature variations reflect both average ambient temperatures on the two test days and variations in ventilation flow

from test to test on a given day as the test operator attempted to maintain a constant test cell temperature. Both fuel comparisions show a similar trend of increased torque variation with the speed. Also the lean mixture settings resulted in increased torque variation compared to the rich mixture settings.

Figures 7 and 8 show cylinder-to-cylinder air-fuel ratio distribution at the different operating points. The standard deviation of air-fuel ratio is listed in table 5. At the lower speed, the variation of the cylinder-to-cylinder mixture distribution was small, but it increased with increased speed and load. The variation for 15B fuel indicated a greater maldistribution compared to 100LL fuel. Maldistribution for 12A fuel was relatively high at 1000 and 1600 rpm and about the same as 100LL at the other points. Of the 4 cylinders, numbers 1 and 3 had the worst maldistribution. Lean mixtures exhibited more maldistribution than rich mixtures. Between the two test days, the inlet air temperature changed about 20° F. The lower ambient temperature corresponded to increased maldistribution with the 100LL fuel as shown in table 5. Based on this limited data, it appears as if inlet air temperature is more influential than fuel volatility on maldistribution in this engine. Additional studies of the effect of inlet air temperature are needed.

TABLE 5. STANDARD DEVIATION OF AIR-FUEL RATIO

Mode	1	2	3	4	5	6	7	8
RPM	1000	1600	2000	2200	2200*	2350	2350*	2700
T_i**	67.5	75	91	65.5	63.5	73.5	66.5	69
100LL	0.22	0.37	0.47	0.57	0.61	0.75	1.03	0.37
15B	0.39	0.21	0.47	0.65	0.79	0.66	0.86	0.69
T_i**	47.5	47.5	51.5	53.5	52.5	51.5	54	53
100LL	0.58	0.43	0.75	1.03	2.10	1.09	1.37	0.50
12A	0.96	0.55	0.33	1.00	1.76	0.99	1.76	0.49

* Lean mixture

** Intake air temperature, ° F

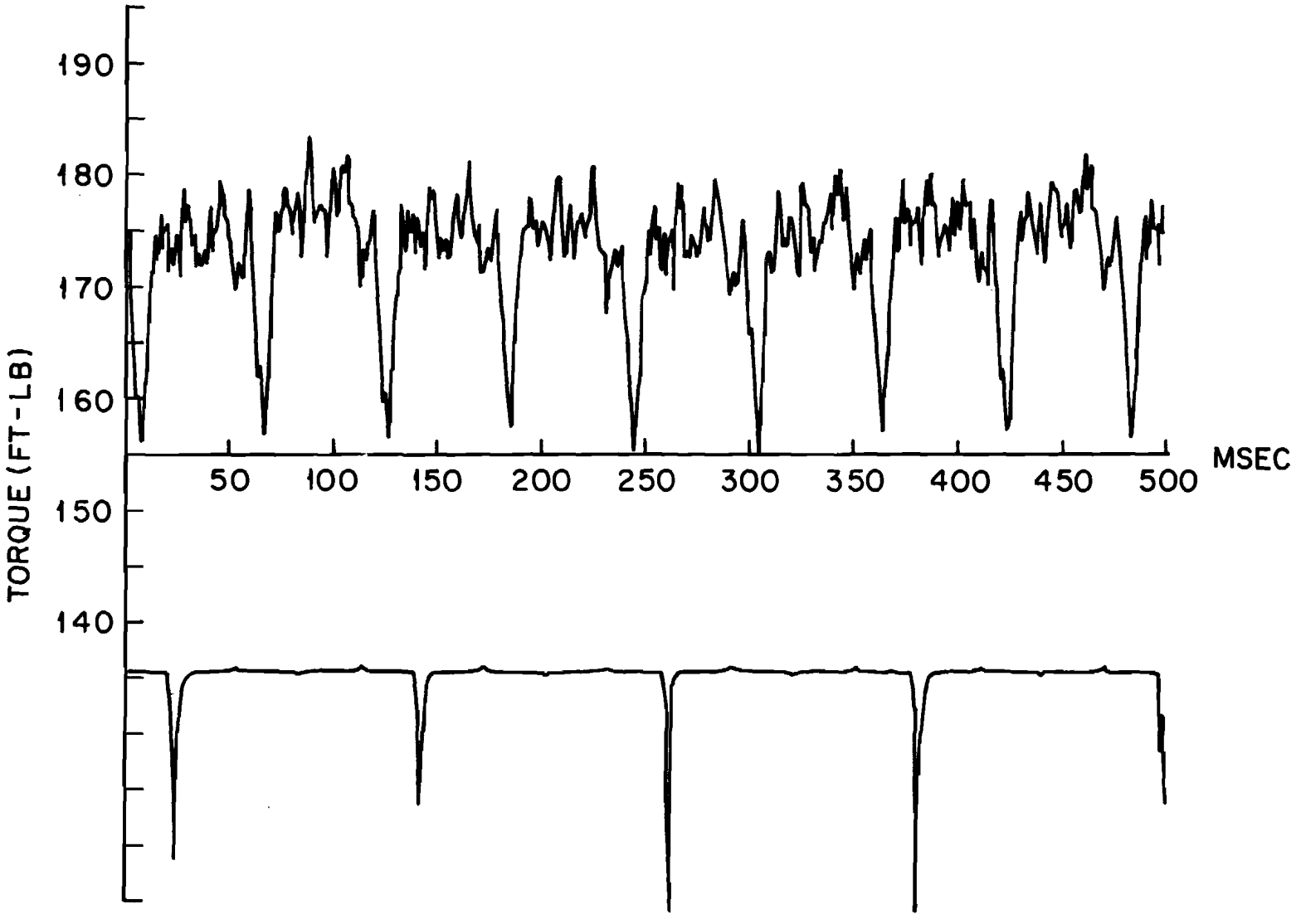

FIGURE 5. TORQUE VARIATION OUTPUT SIGNAL FOR 15B FUEL AT 2000 RPM-UPPER TRACE, IGNITION TIMING-LOWER TRACE

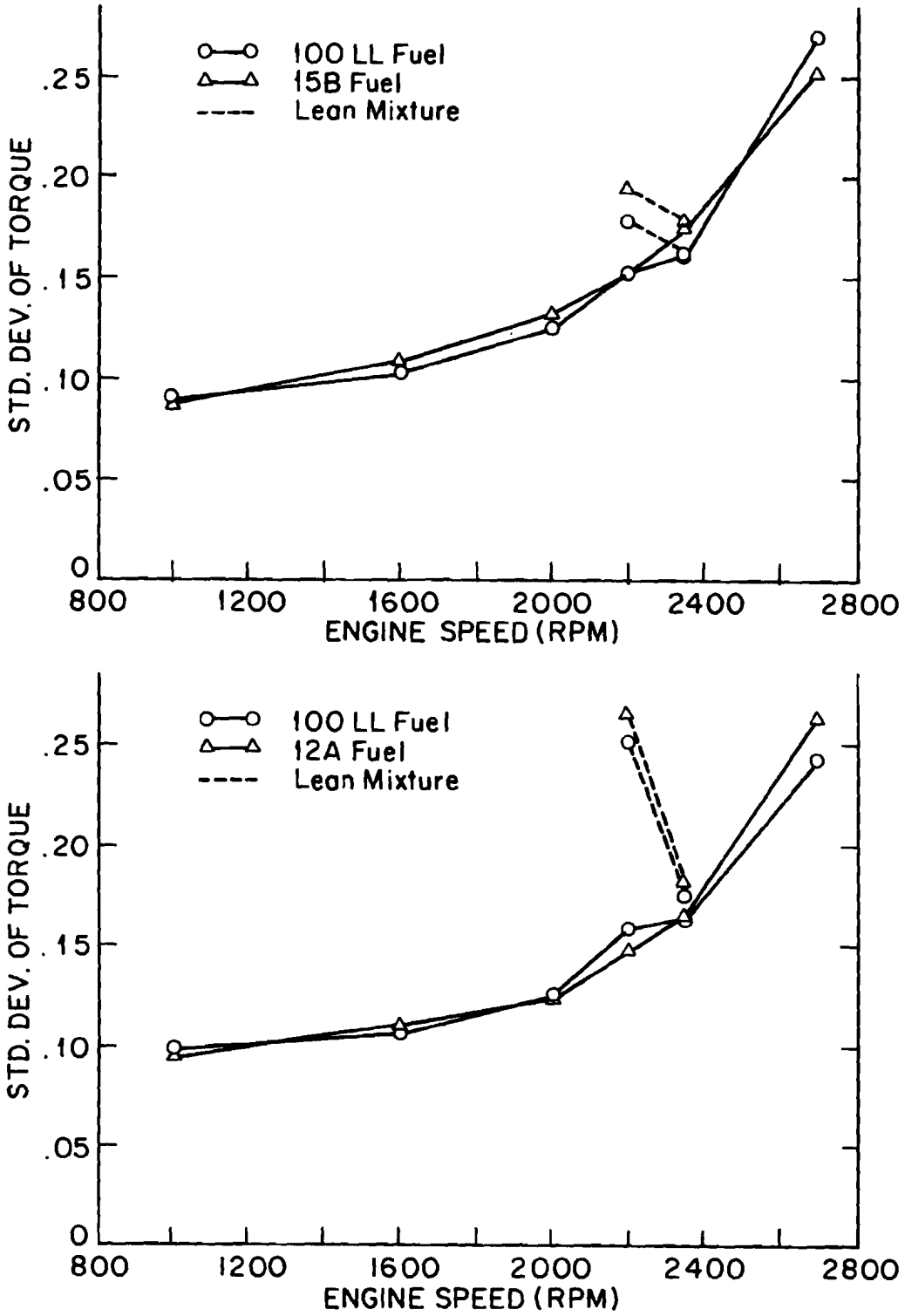

FIGURE 6. STANDARD DEVIATION OF TORQUE VARIATION PRODUCED WITH EACH TEST FUEL

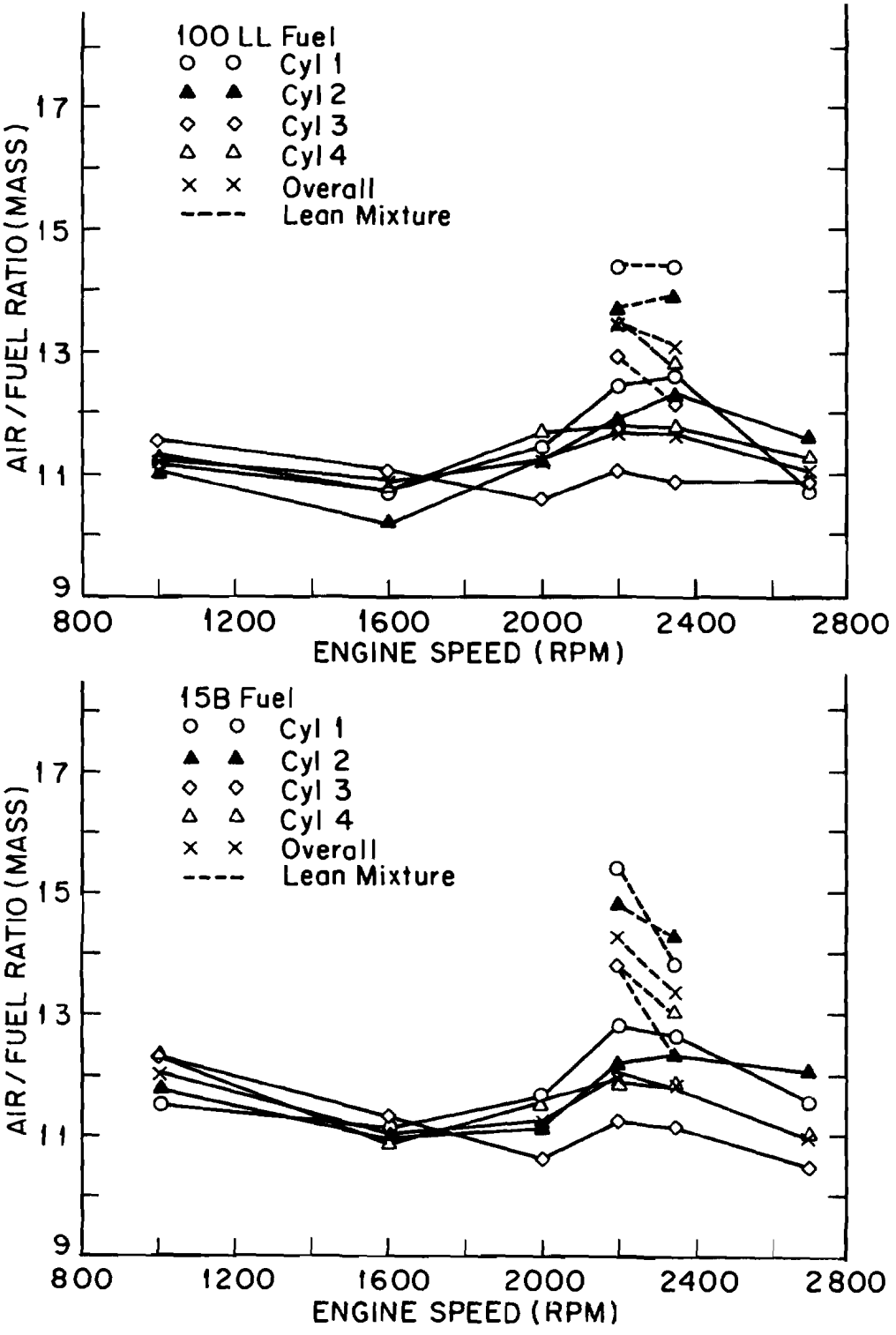

FIGURE 7. AIR-FUEL RATIO DISTRIBUTION WITH BASELINE (100LL) AND TEST FUEL 15B

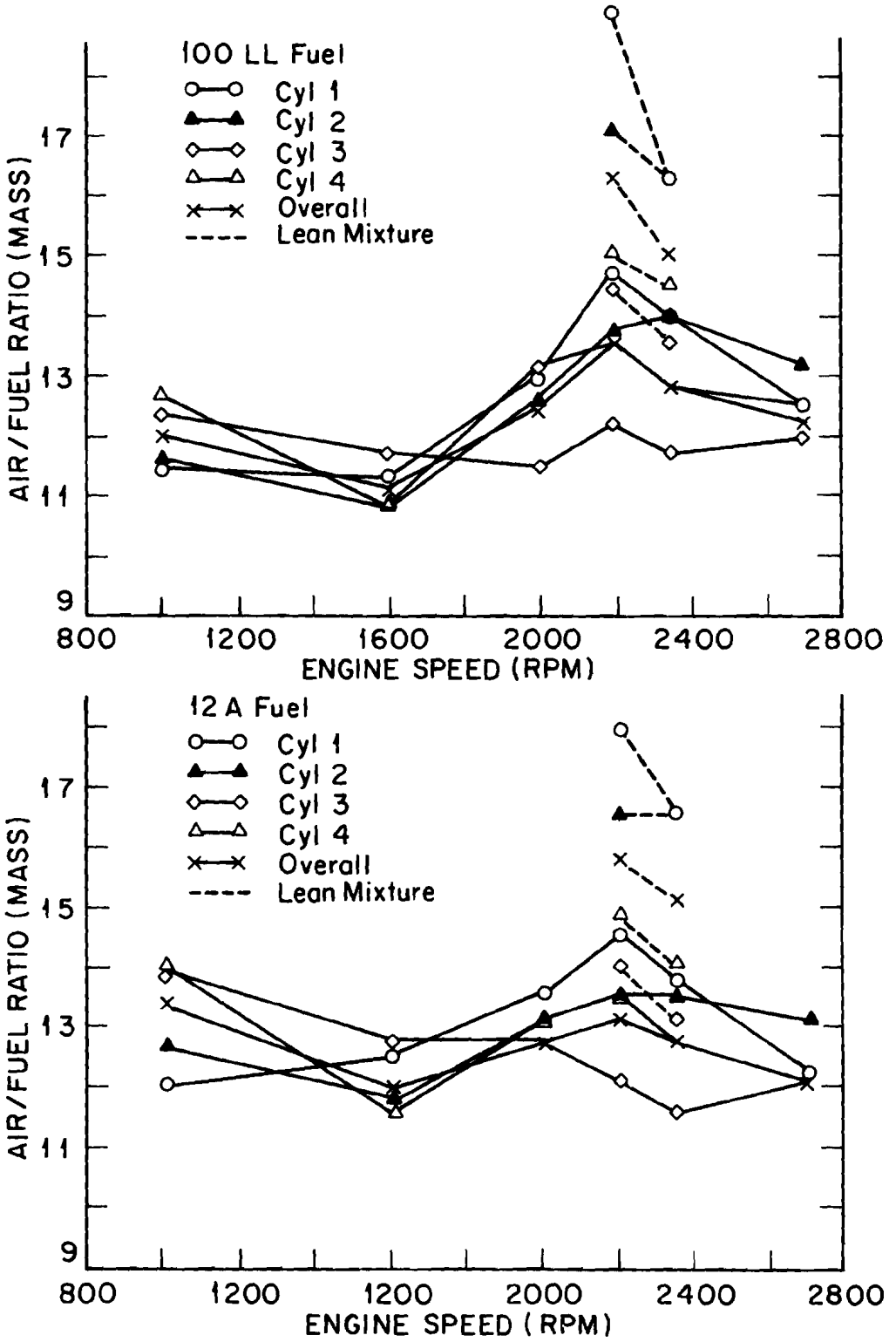

FIGURE 8. AIR-FUEL RATIO DISTRIBUTION WITH BASELINE (100LL) AND TEST FUEL 12A

DISCUSSION

The power of an engine is generated as a result of combustion of the air-fuel mixture. Ideally the engine should have uniform cylinder-to-cylinder air-fuel ratio for smoothest power. However, in actual practice, distribution is not uniform. Sources of maldistribution include the heavy and light components of the fuel. These are indicated by the ASTM 90 percent and 10 percent points. For the Lycoming 0-320 engine used in this experiment, the intake was heated by the oil sump which was about 150° F. Since 15B and 12A fuels have both more light and heavy components than 100LL fuel, they may be expected to produce greater mixture maldistribution. Since this was not the case, it is suggested that the updraft carburetion and heated manifold system on this engine were much more tolerant to widely varying fuel properties than the conventional downdraft automotive system tested by Cooper et al. (reference 5).

As the load and speed increased, the flow rate of fuel and air increased. The greater heat transferred from the air charge for evaporation of the fuel produced a lower temperature in the intake manifold. Since the heat transfer available for evaporation was nearly constant with a fixed manifold area and sump temperature, the distribution became worse as the speed and load increased and charge temperature fell.

The standard deviation of torque in figure 6 shows virtually no effect of volatility. For lean mixtures, the torque variation was significantly higher than for rich mixtures. At the richer mixture of about 12:1, the torque was relatively insensitive to any small variations in air-fuel ratio. On the other hand, at leaner mixtures, the same variation in the air-fuel ratio produced a larger variation in torque. As the load increased, the magnitude of the torque pulses increased and therefore the instantaneous torque variation was increased.

The brake specific fuel consumption rate (BSFC) was calculated from the fuel flowrate and brake horsepower output for each fuel. These values are compared in figure 9. Each fuel gave a similar level of specific fuel economy.

Throttle plate temperatures are shown in figure 10 for the tested fuels along with the intake air temperatures. The lower throttle plate temperatures for both 15B and 12A fuels indicate possible icing problems with high humidity air. In our tests the absolute humidity was 0.0052 lbm/lbm or less (relative humidity 34 percent at 70° F) and at this low level no indication of icing was found.

Potential for vapor formation in a given fuel system is determined by the system pressure and temperature together with the volatility of the fuel. The falling pressure with increased fuel flow characteristic in figure 11 is generally attributable to the pressure drop characteristics of the Brooks fuel flowmeter. However, for equal conditions, the lower pressure in the fuel line for the automobile type fuels compared to

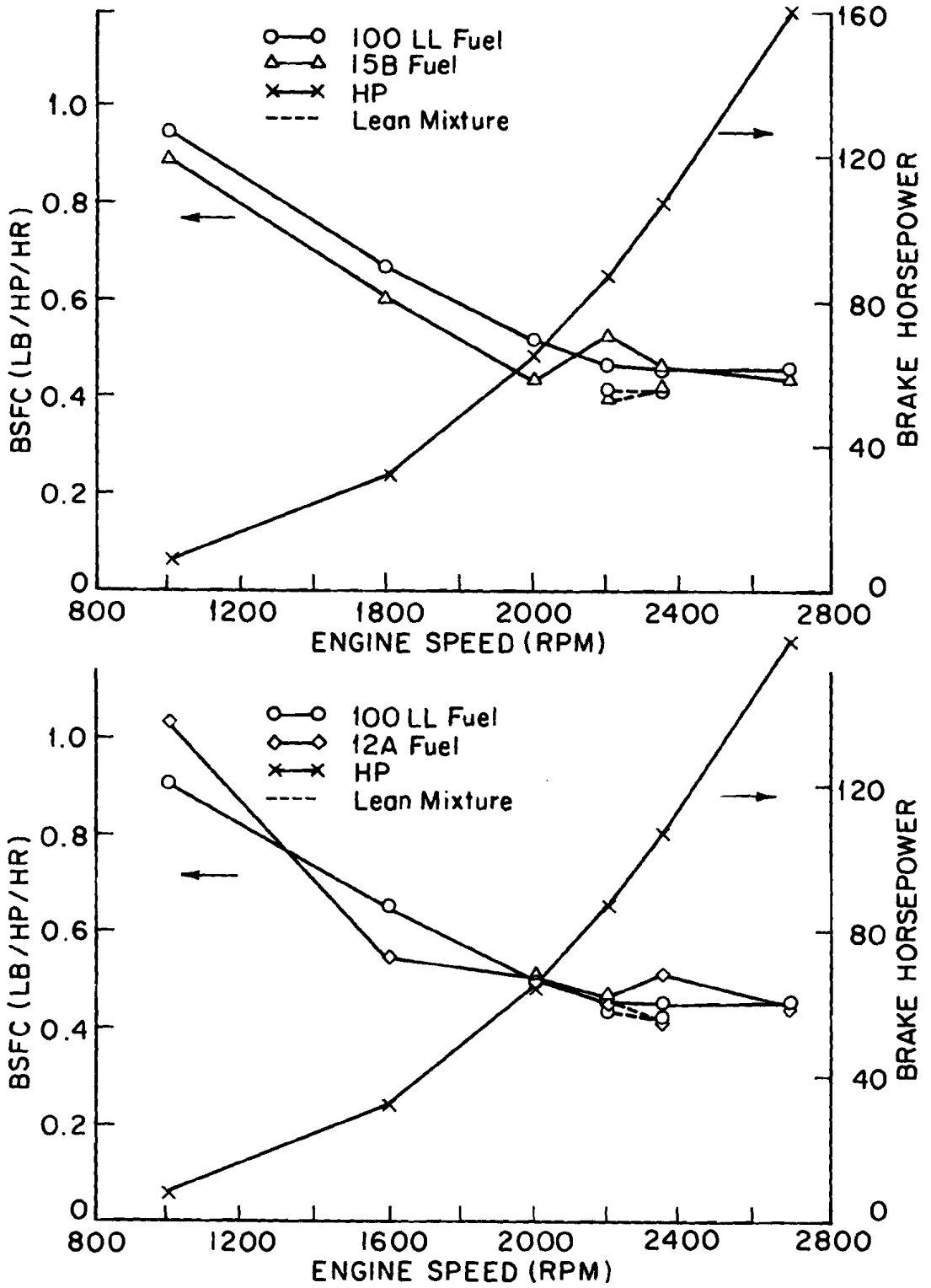

FIGURE 9. BRAKE SPECIFIC FUEL CONSUMPTION RATE WITH EACH FUEL TESTED
Power was set to be the same for each.

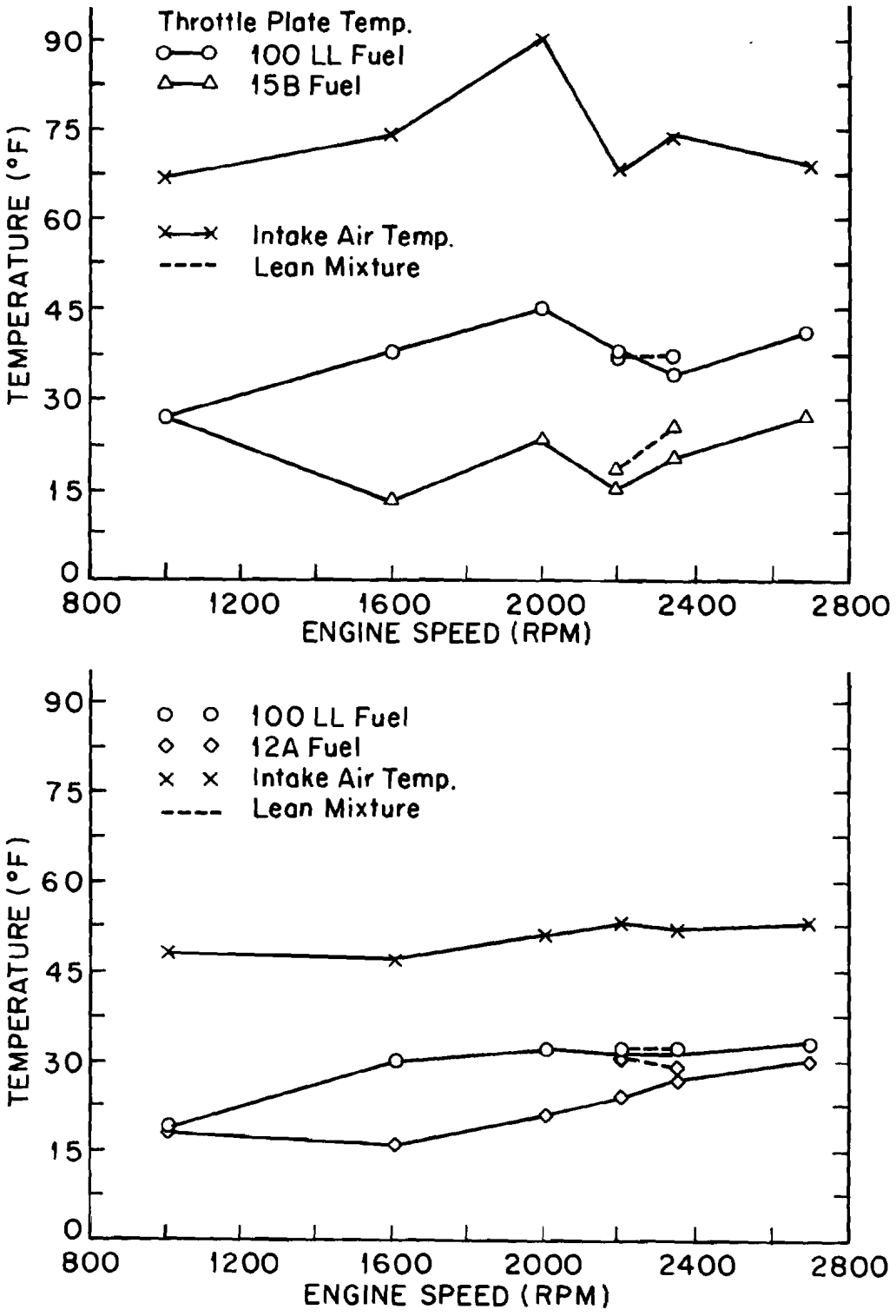

FIGURE 10. THROTTLE PLATE AND INTAKE AIR TEMPERATURE VARIATION WITH EACH FUEL TESTED

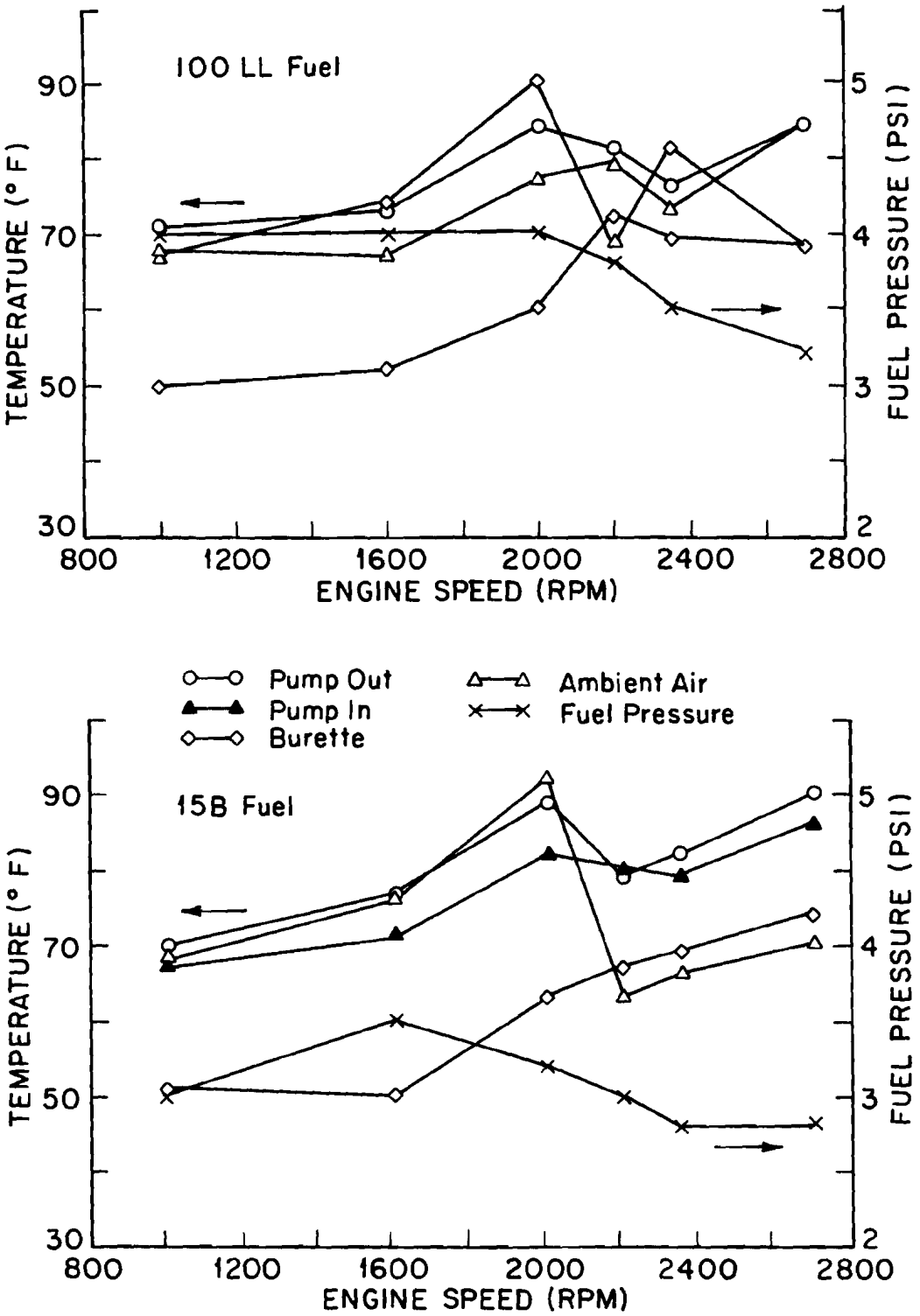

FIGURE 11. FUEL PRESSURE AT THE CARBURETOR AND TEMPERATURE AT VARIOUS LOCATIONS WITH BASELINE (100LL) AND 15B TEST FUEL

100LL fuel is taken to indicate the formation of vapor. Another indication of vapor formation was erratic operation of the Brooks flowmeter which was located between the carburetor and fuel pump. This positive displacement meter indicated more fuel flow than the burette and this has been attributed to vapor formed in the fuel line. Although vapor lock problems were not detected in this experiment, vapor lock might be expected at higher temperature conditions with the volatile fuels.

OBSERVATIONS AND CONCLUSIONS

From the experimental results and observations in this study of the effect of automobile fuels on light aircraft piston engine performance, the following conclusions were drawn for the two automobile fuels compared to 100LL aviation fuel on the Avco Lycoming 0-320 engine:

1. In terms of mixture distribution and power output, both automotive type fuels were similar to commercial 100LL aircraft fuel.

2. The torque fluctuations for all fuels tested were about the same. These were moderate with rich mixtures and relatively high with lean mixtures.

3. Specific fuel consumption was similar for each tested fuel.

4. Based on an observation of torque output, icing was not observed. However, for humid ambient air, the lower temperature at the throttle plate produced with the more volatile fuels can be expected to increase potential icing problems.

5. Vapor formation was detected in this experiment for both automotive fuels. This was evidenced by the lower pressure in the fuel line and increased fuel volume flow in the supply line compared to 100LL. Much more vapor could be expected to evolve at fuel system temperatures higher than those of this test and greater vapor lock problems are projected. No evidence of vapor lock was found with the 100LL fuel at the test conditions run.

6. Cylinders number 1 and 3 exhibited more air-fuel ratio maldistribution than numbers 2 and 4.

REFERENCES

1. Patterson, D. J., Morrison, K., Remondeno, M., and Slopsema, T., "Light Aircraft Engines, the Potential and Problems for Use of Automotive Fuels, Phase 1-Literature Search," U. S. DOT Report, No. FAA-CT-81-150, Dec. 1980.

2. Yu, H. T. C., "Fuel Distribution Studies-A New Look at an Old Problem," SAE Trans. Vol. 71, 1963, pp. 596-613.

3. Bayer, E., "Gas Chromatography," Elsevier Publishing Company, 1961.

4. Donahue, R. W. and Kent, R. H., "A Study of Mixture Distribution," SAE Quarterly Trans. Vol. 4, No. 4, PP. 546-560.

5. Cooper, D. E., Courtney, R. L., and Hall, C. A., "Radioactive Tracers Cast New Light on Fuel Distribution," SAE Trans. Vol. 67, Jan., 1959, PP. 619-639.

6. Mirsky, W. and Nicholls, J. A., "The Influence of Mixture Distribution on Emissions from an Aircraft Piston Engine," U. S. DOT Report, No. FAA-RD-80-122 and FAA-CT-80-62, Oct. 1980.

7. Haslett. R. A. and Eidson, T. M., "Equivalence Ratio Meter," SAE Paper 770219, 1977.

8. Sensors Lamdascan, Air/Fuel Ratio Analyzer Manual, Sensors Inc., Ann Arbor, Mi.

9. Shelton, E. M., "Motor Gasolines, Winter 1978-1979," U. S. DOE Report, No. DOE/BETC/PPS-79, 1979.

10. Shelton, E. M., "Motor Gasolines, Summer 1979," U. S. DOE Report, No. DOE/BETC/PPS-80/1, 1980.

11. Avco Lycoming Operator's Manual for O-320, IO-320, AIO-320 and LIO-320 Series Aircraft Engines, Williamport, PA., 1973.

NOMENCLATURE

A/F	Air-fuel ratio, mass basis
ASTM	American Society for Testing and Materials
FBP	ASTM distillation final boiling point, $^{\circ}$F
H/C	Hydrogen to carbon ratio, mass basis
IBP	ASTM distillation initial boiling point, $^{\circ}$F
MON	Motor octane number
RON	Research octane number
RVP	Reid vapor pressure, psi
TEL	Tetraethyllead antiknock

APPENDIX A

STOICHIOMETRIC AIR-FUEL RATIO CALCULATION

Example for 15B fuel:

H/C (mass) = 0.175

H/C (atom) = 0.175 x 12 = 2.1

15B fuel is represented as $CH_{2.1}$.

Combustion equation for 15B fuel is,

$$CH_{2.1} + (3.05/2)\,O_2 + 3.76\,(3.05/2)\,N_2 \longrightarrow CO_2 + 1.05H_2O + (11.468/2)\,N_2.$$

Air mass: $(3.05/2) \times 32 + (11.468/2) \times 28 = 209.35$

Fuel mass: $12 + 2.1 = 14.1$

Stoichiometric A/F Ratio for 15B fuel = 209.35/14.1

= 14.85

APPENDIX B

DATA COLLECTED FROM EXPERIMENT

Date: 2-11-82
Fuel: 100LL

Ambient Conditions:
Temperature, 19°F
Pressure, 30.17" Hg.
Relative Humidity, 55%

1. Run No.	1	2	3	4	5	6	7	8
2. Avg. Speed - rpm	1000	1620	2000	2200	2200	2350	2350	2700
3. Nom. Torque-lb/ft.	42	105	171	208	208	239	239	311
4. Lebow-Nicolet	7-1	7-3	7-5	7-7	7-8	8-3	8-4	8-7
5. Burette Vol. (cc)	148.4	148.4	299.2	299.2	299.2	608.1	608.1	608.1
6. Burette-min.	1.832	0.649	0.827	0.688	0.774	1.113	1.238	0.740
7. Lamdascan, cyl. 1	28.5	31	27	23	18	22.5	18	31
8. " , cyl. 2	29	35	28	25	19.5	23.5	19	26.5
9. " , cyl. 3	26.5	29	32	29	21.5	30	24	30
10. " , cyl. 4	27.5	31	26	25.5	20	25.5	22	28
11. overall 5	28	30	28	26	20	26	21	29
12. T-°F, exh. man., cyl. 1	1106	1241	1283	1338	1454	1335	1420	1307
13. " " , cyl. 2	1043	1217	1324	1402	1428	1433	1437	1451
14. " " , cyl. 3	1052	1232	1340	1436	1433	1459	1460	1465
15. " " , cyl. 4	1102	1221	1382	1412	1469	1388	1481	1374
16. Oil into cooler 1 - °F	111	126	167	167	158	154	161	175
17. Oil out of cooler 2 -°F	70	84	115	123	120	116	125	118
18. Fuel burette, 3 - °F	50	52	60	72	71	69	60	68
19. Int. man. cyl. 1,5-1, °F	107	79	92	74	71	62	68	58
20. " " cyl. 2,5-2, °F	114	78	89	69	67	59	65	57
21. " " cyl. 3,5-3, °F	100	80	86	65	64	56	60	57
22. " " cyl. 4,5-4, °F	106	79	90	68	65	56	62	57
23. Carb. plate, 5-5, °F	27	38	45	38	37	34	37	41
24. Carb. bowl, 5-6, °F	82	83	92	86	75	79	83	85
25. Fuel pump inlet, 5-7, °F	68	67	77	79	81	73	75	84
26. Fuel pump outlet, 5-8, °F	71	73	84	81	82	76	79	84
27. Oil inside sump, 5-9, °F	109	141	158	153	146	142	147	151
28. Flowmeter, 5-10 - °F	67	74	90	68	65	81	66	68
29. P, int. vac.-in.Hg.	19.4	15.1	9.9	7.4	6.6	5.6	4.5	2.1
30. Lam. flowmeter-in.H_2O	.390	1.060	1.978	2.236	2.324	2.613	2.770	3.623
31. Cooling fan - in. H_2O	1	1	3.4	4.2	4.2	4.2	4.2	5.4
32. Oil pressure - psi	66	77	81	85	86	88	88	94
33. Fuel pressure - psi	4	4	4	3.8	3.4	3.4	4.0	3.2
34. Cyl. Head 1 - °F	238.1	339.2	355.1	368.6	340.8	377.5	357.7	425.8
35. Cyl. Head 2 - °F	257.8	362.0	370.9	381.7	353.8	390.4	373.0	442.7
36. Cyl. Head 3 - °F	238.6	338.7	341.6	352.2	356.6	355.8	381.4	398.7
37. Cyl. Head 4 - °F	253.1	347.2	355.2	358.1	331.9	367.5	381.7	408.5
38. Act. A/F Ratio, Cyl. 1	11.14	10.72	11.44	12.44	14.40	12.60	14.40	10.72
39. " " " , Cyl. 2	11.05	10.19	11.24	11.90	13.70	12.30	13.92	11.55
40. " " " , Cyl. 3	11.55	11.05	10.57	11.05	12.93	10.88	12.16	10.88
41. " " " , Cyl. 4	11.34	10.72	11.66	11.77	13.49	11.77	12.76	11.14
42. Overall Total A/F ratio	11.24	10.88	11.24	11.66	13.49	11.66	13.11	11.05
43. Torque-HP	8	32	65	87	87	107	107	160

Date: 2-11-82

Fuel: 15B

Ambient Conditions:
Temperature, 19°F
Pressure, 30.17" Hg.
Relative Humidity, 55%

1. Run No.	1	2	3	4	5	6	7	8
2. Avg. Speed - rpm	1000	1620	2000	2200	2200	2350	2350	2700
3. Nom. Torque-lb/ft.	42	105	171	208	208	239	239	311
4. Lebow-Nicolet	7-2	7-4	7-6	8-1	8-2	8-5	8-6	8-8
5. Burette Vol. (cc)	144	144	296	296	296	590	590	590
6. Burette-sec.	113.3	41.8	58.7	36.1	48.1	66.5	73.5	47.3
7. Lamdascan, cyl. 1 (mv)	26	28	25.5	21.5	10	22	19	26
8. " , cyl. 2	25	29	28	23.5	17	23	18	24
9. " , cyl. 3	23	27	31	27.5	19	28	23	32
10. " , cyl. 4	23	29.5	26	24.5	19	25	21	29
11. overall 5	24	28.5	27.5	24.0	18	25	20	29
12. T-°F, exh. man., cyl. 1	1106	1276	1303	1350	1454	1358	1450	1327
13. " " , cyl. 2	1059	1267	1345	1410	1391	1442	1425	1433
14. " " , cyl. 3	1070	1272	1370	1448	1419	1409	1445	1445
15. " " , cyl. 4	1141	1255	1383	1422	1455	1426	1501	1408
16. Oil into cooler 1-°F	110	151	167	155	156	163	166	184
17. Oil out of cooler 2- °F	74	94	117	98	111	124	127	97
18. Fuel burette, 3- °F	51	50	63	67	79	69	79	74
19. Int. man. cyl. 1,5-1, °F	105	91	94	69	71	69	73	68
20. " " cyl. 2,5-2, °F	111	90	91	66	69	67	71	66
21. " " cyl. 3,5-3, °F	100	90	89	65	68	66	69	66
22. " " cyl. 4,5-4, °F	106	90	91	66	66	66	69	67
23. Carb. plate, 5-5, °F	27	13	23	15	18	20	25	27
24. Carb. bowl, 5-6, °F	83	86	94	81	85	84	85	90
25. Fuel pump inlet, 5-7, °F	67	71	82	80	86	79	87	86
26. Fuel pump outlet, 5-8, °F	170	77	89	79	83	82	88	90
27. Oil inside sump, 5-9, °F	109	151	159	143	144	148	151	159
28. Flowmeter, 5-10 -°F	68	76	92	63	62	66	67	70
29. P, int. vac.-in.Hg.	19.5	15.2	10.0	7.8	5.8	5.4	4.2	2.1
30. Lam. flowmeter-in.H_2O	.404	1.057	1.934	2.148	2.450	2.604	2.765	3.585
31. Cooling fan in.H_2O	1	1	3.4	4.2	4.2	4.2	4.2	5.4
32. Oil pressure - psi	65	74	81	86	86	88	88	94
33. Fuel pressure - psi	3	3.5	3.2	3	3.1	2.8	3.0	2.8
34. Cyl. Head 1 - °F	234.6	353.7	361.2	359	314.8	387.9	357.6	430.6
35. Cyl. Head 2 - °F	254.7	378	375.3	372.3	339.1	401.2	377.2	448.9
36. Cyl. Head 3 - °F	236.4	350	345.5	347.0	348.9	370.8	384.1	392.1
37. Cyl. Head 4 - °F	251.6	354.8	357.7	353.4	342.1	379.9	385.3	412.1
38. Act. A/F Ratio, Cyl. 1	11.53	11.12	11.65	12.79	15.37	12.62	13.77	11.53
39. " " " , Cyl. 2	11.77	10.93	11.12	12.17	14.77	12.31	14.24	12.03
40. " " " , Cyl. 3	12.31	11.32	10.61	11.22	13.77	11.12	12.31	10.46
41. " " " , Cyl. 4	12.31	10.85	11.53	11.90	13.77	11.77	12.97	10.93
42. Overall Total A/F ratio	12.03	11.02	11.22	12.03	14.24	11.77	13.35	10.93
43. Torque-HP	8	32	65	87	87	107	107	160

Date: 2-19-82

Fuel: 100LL

Ambient Conditions:
Temperature, 33°F
Pressure 29.98" Hg.
Relative Humidity 95%

1. Run No.	1	2	3	4	5	6	7	8
2. Avg. Speed - rpm	1000	1620	2000	2200	2200	2350	2350	2700
3. Nom . Torque-lb/ft.	42	105	171	208	208	239	239	311
4. Lebow-Nicolet	9-1	9-3	9-5	9-7	10-1	10-3	10-6	10-7
5. Burette Vol. (cc)	148.4	148.4	299.2	299.2	299.2	508.1	608.1	608.1
6. Burette-min.	1.908	.666	.856	.705	.735	1.130	1.210	.752
7. Lamdascan, cyl. 1	26.8	27.7	21.5	17.5	12	19	15	23
8. " , cyl. 2	26.1	30.5	22.5	19.5	14	19	15	21
9. " , cyl. 3	23.3	25.8	27	24	18	26	20	25
10. " , cyl. 4	22.2	30.3	21.	20	17	22	18	23
11. overall 5	24.5	28.3	23	20	15	22	17	24
12. T-°F, exh. man., cyl. 1	1090	1234	1259	1318	1462	1332	1412	1352
13. " " , cyl. 2	1020	1195	1297	1398	1401	1439	1407	1416
14. " " , cyl. 3	1042	1226	1352	1456	1464	1469	1448	1395
15. " " , cyl. 4	1085	1207	1373	1424	1469	1418	1471	1403
16. Oil into cooler 1 - °F	100	104	140	141	151	154	154	156
17. Oil out of cooler 2 - °F	76	78	94	98	103	114	100	110
18. Fuel burette, 3 - °F	72	70	76	74	76	76	82	70
19. Int. man. cyl. 1,5-1, °F	88	50	56	55	59	54	56	47
20. " " cyl. 2,5-2, °F	96	49	54	51	55	51	54	44
21. " " cyl. 3,5-3, °F	83	52	51	50	53	50	51	46
22. " " cyl. 4,5-4, °F	90	52	56	51	52	50	51	46
23. Carb. plate, 5-5, °F	19	30	32	31	32	31	32	33
24. Carb. bowl, 5-6, °F	73	76	82	81	83	81	83	80
25. Fuel pump inlet, 5-7, °F	77	77	83	82	85	80	88	77
26. Fuel pump outlet, 5-8, °F	74	76	83	83	86	83	86	81
27. Oil inside sump, 5-9, °F	97	104	134	132	139	140	138	134
28. Flowmeter, 5-10 - °F	48	47	51	53	53	52	54	53
29. P, int. vac.-in.Hg.	19.4	15.5	10.9	7.6	4.7	5.4	4.0	2.0
30. Lam. flowmeter-in.H_2O	.349	1.005	1.654	2.172	2.529	2.560	2.773	3.555
31. Cooling fan- in H_2O	1.1	1.1	3.3	3.3	3.3	3.3	4.1	5.8
32. Oil pressure - psi	64	75	83	87	87	88	89	94
33. Fuel pressure - psi	3.0	3.4	3.4	3.0	3.0	3.0	3.0	3.0
34. Cyl. Head 1 - °F	207.9	294.1	325.6	362.0	306.8	393.6	335.8	397.1
35. Cyl. Head 2 - °F	227.0	316.2	343.8	380.4	350.1	408.3	345.3	426.4
36. Cyl. Head 3 - °F	207.4	289.3	301.5	336.7	359.9	363.7	372.9	383.0
37. Cyl. Head 4 - °F	222.7	299.8	324.9	357.3	357.8	379.1	375.5	397.7
38. Act. A/F Ratio, Cyl. 1	11.48	11.30	12.93	14.66	18.98	13.92	16.22	12.44
39. " " " , Cyl. 2	11.64	10.80	12.60	13.70	17.01	13.92	16.22	13.11
40. " " " , Cyl. 3	12.36	11.70	11.44	12.16	14.40	11.66	13.49	11.90
41. " " " , Cyl. 4	12.69	10.83	13.11	13.49	14.93	12.76	14.40	12.44
42. Overall Total A/F Ratio	12.02	11.14	12.44	13.49	16.22	12.76	14.93	12.16
43. Torque - HP	8	32	65	87	87	107	107	160

Date: 2-19-82

Fuel: 12A

Ambient Conditions:
Temperature, 33°F
Pressure, 29.98" Hg.
Relative Humidity 95%

1. Run No.	1	2	3	4	5	6	7	8
2. Avg. Speed - rpm	1000	1620	2000	2200	2200	2350	2350	2700
3. Nom. Torque-lb/ft.	42	105	171	208	208	239	239	311
4. Lebow-Nicolet	9-2	9-4	9-6	9-8	10-7	10-4	10-5	10-8
5. Burette Vol. (cc)	144	144	296	296	296	590	590	590
6. Burette- sec.	102.2	48.5	52.8	43.6	43.6	63.4	77.3	52.5
7. Lamdascan, cyl. 1	23.3	21.7	19	17	12.5	18.5	14	22.5
8. " , cyl. 2	21.2	24	20	19	14	19	14	20
9. " , cyl. 3	18.3	21	21	23	18	25	20	23
10. " , cyl. 4	18.0	25	20	19	16.5	21	18	23
11. overall 5	19.4	23.5	21	20	15	21	16	23
12. T-°F, exh. man., cyl. 1	1185	1282	1273	1333	1473	1346	1429	1403
13. " " , cyl. 2	1090	1246	1326	1416	1393	1458	1403	1446
14. " " , cyl. 3	1091	1285	1386	1466	1459	1484	1436	1426
15. " " , cyl. 4	1170	1257	1387	1450	1473	1444	1513	1436
16. Oil into cooler 1-°F	97	128	139	149	148	161	153	171
17. Oil out of cooler 2-°F	70	87	81	100	107	110	118	106
18. Fuel burette, 3 - °F	72	73	74	73	76	74	86	73
19. Int. man. cyl. 1,5-1, °F	84	63	60	59	58	57	61	54
20. " " cyl. 2,5-2, °F	92	63	56	56	54	56	59	52
21. " " cyl. 3,5-3, °F	81	65	56	55	51	55	58	54
22. " " cyl. 4,5-4, °F	87	64	59	58	52	57	59	54
23. Carb. plate, 5-5, °F	18	16	21	24	31	27	29	30
24. Carb. bowl, 5-6, °F	71	81	80	81	82	83	81	83
25. Fuel pump inlet, 5-7, °F	75	85	84	85	85	88	81	89
26. Fuel pump outlet, 5-8, °F	72	83	83	85	86	88	83	85
27. Oil inside sump, 5-9, °F	92	123	130	136	137	144	139	141
28. Flowmeter, 5-10 - °F	47	48	52	54	52	51	54	53
29. P, int. vac.-in.Hg.	19.4	15.5	10.9	7.3	4.6	5.3	4.0	2.0
30. Lam. flowmeter-in.H_2O	.379	1.061	1.654	2.172	2.529	2.543	2.775	3.494
31. Cooling fan - in. H_2O	1.1	1.1	3.3	3.3	3.3	3.3	4.1	5.8
32. Oil pressure - psi	65	75	84	87	88	88	89	94
33. Fuel pressure - psi	3.0	2.7	2.8	3.1	3.0	2.7	2.9	2.8
34. Cyl. Head 1 - °F	205.1	309.0	328.8	363.0	307.2	398.4	335.0	401.2
35. Cyl. Head 2 - °F	222.7	332.2	344.4	384.8	348.2	409.8	344.0	431.0
36. Cyl. Head 3 - °F	205.9	299.4	301.8	341.0	363.8	364.9	373.2	394.7
37. Cyl. Head 4 - °F	218.2	312.2	326.1	364.1	357.1	382.3	375.5	400.7
38. Act. A/F Ratio, Cyl. 1	12.04	12.53	13.57	14.55	17.96	13.79	16.58	12.28
39. " " " , Cyl. 2	12.70	11.85	13.15	13.57	16.58	13.57	16.58	13.15
40. " " " , Cyl. 3	13.89	12.77	12.77	12.13	14.03	11.60	13.15	12.13
41. " " " , Cyl. 4	14.03	11.60	13.15	13.57	14.84	12.77	14.03	12.13
42. Overall total A/F Ratio	13.39	11.99	12.77	13.15	15.81	12.77	15.14	12.13
43. Torque - HP	8	32	65	87	87	107	107	160.

☆ U.S. GOVERNMENT PRINTING OFFICE: 1983—605-072/21